Mutation and Modeling Analysis of the *Saccharomyces cerevisiae* Swi6 Ankyrin Repeats†

Sandra P. Ewaskow,‡ Julia M. Sidorova,‡ Jörg Hendle,‡,§ J. Craig Emery,|| Deborah E. Lycan,|| Kam Y. J. Zhang,‡ and Linda L. Breeden*,‡

Division of Basic Sciences, Fred Hutchinson Cancer Research Center, Seattle, Washington 98109, and Department of Biology, Lewis and Clark College, Portland, Oregon 97219

Received October 24, 1997; Revised Manuscript Received January 20, 1998

ABSTRACT: The Swi4−Swi6 family of transcription factors confers G1/S specific transcription in budding and fission yeast. These proteins contain four ankyrin repeats, which are present in a large number of functionally diverse proteins and have been shown to be important for protein−protein interaction. However, no specific sequence has been identified that is diagnostic of an ankyrin repeat-interacting protein. To determine the function of the ankyrin repeats of Swi6, we generated both random and site-directed mutations within the ankyrin repeat domain of Swi6 and assayed the transcriptional function of these mutant *swi6* alleles. We found six single mutations, scattered within the first and the fourth repeats, that generate a temperature-sensitive Swi6 protein. In addition, we found that alanine substitutions for the most conserved residues in each repeat were highly deleterious and also confer temperature sensitivity. Most of these *swi6* alleles are able to form ternary complexes with Swi4 and DNA, but these complexes display reduced mobility in band-shift gels, suggesting a dramatic conformational change. We have modeled the ankyrin repeats of Swi6 using the coordinates derived for 53BP2 and find that, despite its low level of sequence conservation, these modeling studies and our mutation data are consistent with Swi6 having a structure very similar to that of 53BP2. Moreover, all but one of our single mutants and all of the site-directed mutants disrupt critical structural features of the predicted folding pattern of these repeats. We conclude that the ankyrin repeats play a major structural role in Swi6. Ankyrin repeats are unlikely to have inherent protein or DNA binding properties. However, they form a characteristic and stable structure with surfaces that may be tailored for many different macromolecular interactions.

The ankyrin−Swi6−Cdc10 repeat was first identified in a family of yeast transcription factors (*1*, *2*). Included within this family are the *Schizosaccharomyces pombe* transcription factors Cdc10, Res1, and Res2 and the *Saccharomyces cerevisiae* transcription factors Swi6, Swi4, and Mbp1 (Figure 1). Members of these groups associate with one another through their C termini (*3*, *4*). The target genes for these transcription factors are expressed at the G1/S transition in yeast and include DNA synthesis genes (*5*, *6*), *HO* endonuclease (*7*), and the G1 cyclins (*8*, *9*) that are required for progression through the yeast mitotic cell cycle. Swi6 is one of the transcription factors that regulates gene expression during G1/S, either as a complex with Mbp1, with which it binds MCB [*Mlu*I cell cycle box (ACGCGTNA)] DNA elements (*5*, *6*, *10*), or in combination with Swi4, with which it binds SCB [*SWI4/6*-dependent cell cycle box (CACGAAAA)] elements (*11*−*13*) as well as MCB-like elements (*14*). Swi6 is not known to bind DNA directly; rather, both Mbp1 and Swi4 confer the DNA binding ability to the complex through their N termini.

A common central motif consisting of four ankyrin repeats is present among all the known G1/S specific yeast transcription factors. Ankyrin repeats typically occur as four or more continuous copies of a 33-amino acid sequence characterized by the consensus sequence ----t--G-o-LHϕAϕ--tt-x$\phi\phi$x-LLx-t-- (Figure 1), where t indicates a residue frequently found in turns, x a polar residue, ϕ a hydrophobic residue, o a serine or threonine residue, and capital letters indicate highly conserved amino acids (*15*). A further defining feature of the yeast transcription factor ankyrin repeats is the central core region, denoted by the consensus sequence G-T-L (Figure 1). Ankyrin repeats are present in a large number of functionally diverse proteins and have traditionally been considered sites of protein−protein interaction. Circular dichroism and NMR studies of the tumor suppressor protein $p16^{INK4A}$, which consists of four ankyrin repeats, have confirmed the predominantly α-helical nature of the ankyrin repeat region (*16*). The crystal structure of the p53 core domain bound to 53BP2 reveals that a single ankyrin repeat structurally consists of one β-hairpin and two α-helices (*17*).

† This work was supported by NIH Grant GM41073 (L.L.B.), DOD Grant DAMD-17-94-J-4122 (L.L.B.), NIH Grant GM50995 (D.E.L.), the Fred Hutchinson Cancer Research Center (J.H. and K.Y.J.Z.), NIH Grant R29GM55663 (J.H. and K.Y.J.Z.), the College of American Pathologists Foundation (S.P.E.), National Research Service Award CA-T32-CA09657 (S.P.E.), and NIH Grant CA-K11-69434 (S.P.E.).

* To whom correspondence should be addressed: Fred Hutchinson Cancer Research Center, Division of Basic Sciences, A2-168, 1100 Fairview Ave. N., Seattle, WA 98109-1024. Phone: (206) 667-4484. Fax: (206) 667-6526. E-mail: lbreeden@fhcrc.org.

‡ Fred Hutchinson Cancer Research Center.

§ Present address: EMBL Hamburg Outstation, c/o DESY, Bldg. 25A, Notkestrasse 85, D-22603 Hamburg, Germany.

|| Lewis and Clark College.

S0006-2960(97)02652-4 CCC: $15.00
Published on Web 03/12/1998

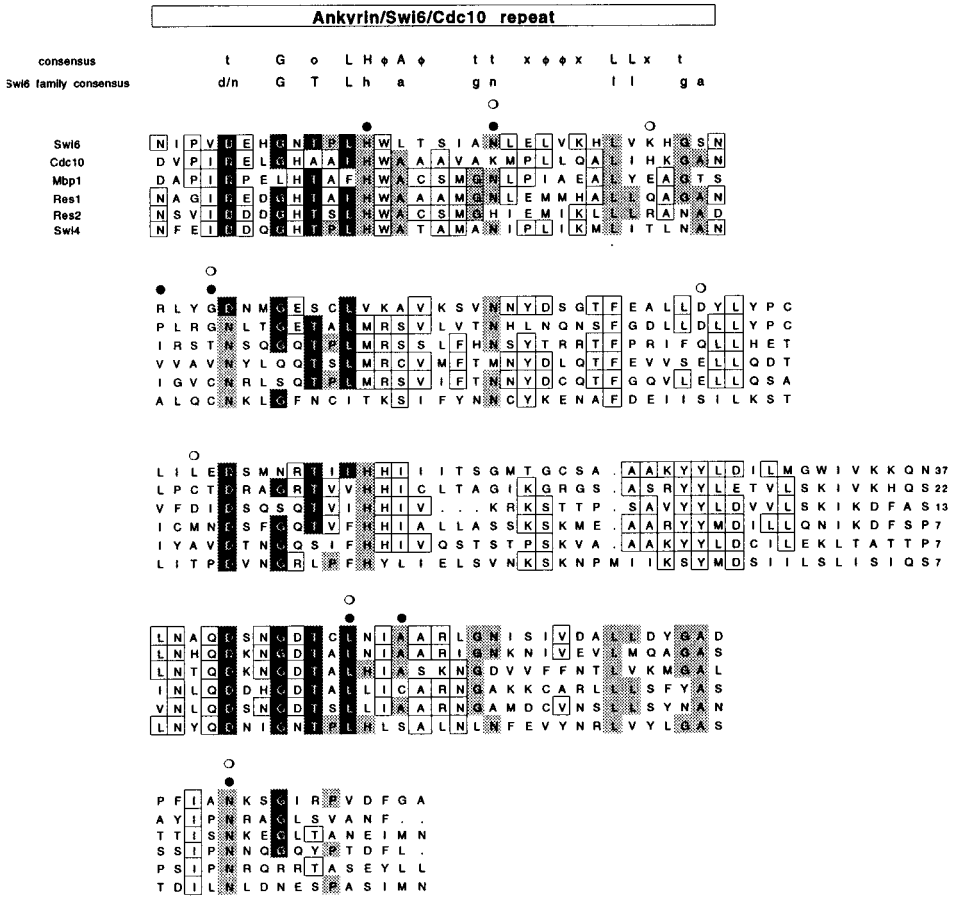

FIGURE 1: Alignment of the ankyrin repeat regions of a family of yeast transcription factors. These three *S. cerevisiae* and three *S. pombe* transcription factors all contain a centrally located ankyrin repeat domain that consists of four full ankyrin repeats and vestiges of a fifth that are tandemly arranged. The black boxes are situated at the most highly conserved residues within the ankyrin motif, known as the "core" region. Each of the ankyrin repeats within the transcription factors has these regions conserved to some degree. The light gray boxes denote residues that are conserved across more than one repeat within this family, and the white boxes highlight residues that are conserved within only one repeat of the ankyrin domain. (●) Single residue substitutions at these sites confer a temperature-sensitive phenotype to Swi6. (○) Mutants with residue substitutions at these locations were isolated more than once. x depicts a polar residue. ϕ depicts a hydrophobic residue. t depicts a residue found in turns.

Ankyrin repeats play an important role in Swi6, Swi4, and Cdc10 function. In Swi6, alanine substitutions of the first and fourth ankyrin repeat core residues result in decreased SCB binding and loss of transcriptional activation by the Swi4−Swi6 complex (*3*). In *cdc10*, the *S. pombe* homologue of *SWI6*, a group of conditional alleles were sequenced and the mutations clustered within the ankyrin repeat domain (*18*). Many of these single mutations mapped to the highly conserved ankyrin repeat core residues of the first and fourth ankyrin repeats. The ankyrin repeat domain of Swi4 is known to interact with the Clb2−Cdc28 kinase (*19*), and this has been postulated to inhibit Swi4−Swi6 transcriptional activity at SCB elements during the G2/M phase of the cell cycle.

The original alignment of Swi6 with other ankyrin repeat-containing proteins showed two repeats with high homology to the *Notch* and *lin-12* repeats, and these were used to define this 33-amino acid repeat (*1*). However, the identification of many more proteins containing ankyrin repeats, and the alignment of the five other members of the Swi4−Swi6 family of transcription factors, makes it clear that ankyrin repeats can be highly degenerate tandemly arranged sequences, and the Swi6 family may contain four full repeats followed by the N-terminal half of a fifth repeat (Figure 1) (*20*).

To determine if all of the Swi6 ankyrin repeats are important for Swi6 transcriptional activation, we used error-prone PCR to mutagenize the ankyrin domain of Swi6. Mutant plasmids were then tested for the ability of altered Swi6 proteins to activate SCB-regulated transcription. We obtained six single mutants and many mutants with combinations of double or triple amino acid residue substitutions that inactivate Swi6 as measured by the blue-white plate assay (*21*) for transcription of the *HO* promoter at permissive (25 °C) and nonpermissive (37 °C) temperatures. In addition, we made site-directed mutations of the most highly conserved residues within the core regions of each of the repeats. These also result in temperature sensitivity and confer band-shift mobility patterns that suggest an important structural role for each of the four repeats. To better understand the structural consequences of these ankyrin repeat mutations, we modeled the Swi6 ankyrin repeat region, using the coordinates obtained from the crystal structure of the four ankyrin repeats of 53BP2 (*17*), and found that Swi6 can adopt a very similar structure. The alanine substitutions in the conserved core leucines are likely to disrupt the regular secondary structure of the ankyrin repeat domain. Five of the six point mutants examined also disrupt the modeled structure, and the sixth mutant resides on the surface of the protein and may define a site of interaction.

EXPERIMENTAL PROCEDURES

PCR Mutagenesis of the Swi6 Ankyrin Repeats. Oligonucleotide primers BL58 (2.5 μM) (5′CCTGTAGATGAGCATGG3′) and BL202 (2.5 μM) (5′CCAAAATCCACGGGTCT3′) were used to perform mutagenic PCR in the presence of 5.0 mM deoxynucleotide triphosphate and either 0.5 mM (screen 1), 0.25 mM (screen 2), or 0.1 mM (screen 2) manganese chloride to facilitate nucleotide misincorporation (*22*). A *SWI6 CEN URA3*+ plasmid pBD1378 (0.05 μM) (*23*) was the double-stranded DNA template. To produce single-stranded templates from the double-stranded mutagenized PCR product, 25 rounds of PCR were performed using kinased primer BL202 (2.5 μM) and 1 μL of the double-stranded mutagenized PCR library product in a 50 μL reaction volume. The resulting single-stranded mutagenized product was then annealed to a single-stranded *SWI6* DNA template produced in the *dut*− *ung*− *Escherichia coli* strain (*24*). The heteroduplex plasmids were then introduced into a *dut*+ *ung*+ *E. coli* strain to propagate, generating the high (0.5 mM $MnCl_2$), middle (0.25 mM $MnCl_2$), and least (0.1 mM $MnCl_2$) mutagenized libraries. We isolated the mutagenized plasmids from *E. coli* using the alkaline plasmid prep procedure (*25*) and then introduced the plasmids into the *swi6* deletion strain BY600 (*MATa, ho:lacZ, swi6::TRP1*−*197, ura3, leu2*−*3,112, ade2, trp1, his3, trp1*−*1, can1*−*100, met*) using the lithium acetate method of transformation (*26*) and isolated those mutants that grew on uracil-deficient agar. Strains bearing the mutant *swi6* alleles were constructed by targeted integration (*27*) of the BY600 strain with linearized pRS305 plasmids carrying the *Hin*dIII−*Sma*I fragments of *swi6*. Both rich (YEPD) and minimal, selective (YC) growth conditions were as described previously (*28*).

Generation of Site-Directed Mutants. Mutant plasmids pBD1819 and pBD1822 were generated from a *Sac*I digest of pBD1028 and pBD1029, respectively, followed by ligation of the 1.5 kilobase fragment into the *Sac*I-digested pRS316. The remainder of the site-directed mutants were generated through substitution of the indicated core residues using oligonucleotide-directed mutagenesis of a single-stranded *SWI6* template (pBD1378) (*24*). The first ankyrin core region was mutated using primer Bd1035 (mutant base pairs are underlined) (5′GCTATTGAAGTTAACCAATGTGCTGGTGCGTTTGCGTGCTCATCTAC3′), the second using primer BL86 (5′GCTTTCACTGCGCATGCCTCCGCCATATTATCACC3′), the third using primer BL87 (5′GATATGGTGCGCAATTGCTCTAGCCATTGAGTCTTC3′), and the fourth using primer Bd1036 (5′GCTGCAATGTTAGCGCAAGCATCGGCATTCGAGTCCTGC3′).

Identification of the Temperature-Sensitive Mutant Plasmids. BY600 (*swi6::TRP1*−*197, ho:lacZ*) was transformed with the PCR-generated libraries and grown on YC-ura plates at 25 °C, then replica plated, and grown at both 25 and 37 °C. The colonies were transferred to nitrocellulose filters and assayed for β-galactosidase activity as described (*21*). The *ho:lacZ* reporter construct for the blue-white screen has been described previously (*21*). Transformants that were blue at 25 °C and white at 37 °C were selected, as well as cells bearing null alleles, which were white at both 25 and 37 °C. Mutant plasmids were then isolated from the yeast strain and retransformed into the BY600 (*swi6::TRP1*−*197*) strain to confirm the dependence of the temperature-sensitive blue-white phenotype on the plasmid-borne *swi6* gene.

To identify mutant plasmids that had significant defects in Swi6 protein stability, extracts were prepared from the temperature-sensitive *swi6* mutants after incubation at 37 °C for 10−12 h. The differences in Swi6 levels are pronounced in some cases and could be contributing to the defective phenotype of ankyrin repeat mutants. Thus, the temperature-sensitive mutants that were selected for further characterization were those which maintain near wild-type levels of Swi6 protein and are likely defective due to a loss of function at high temperatures.

Generation of Yeast Strains. Yeast strains BY2214 through BY2223 were generated by ligating the 2.8 kilobase *Hin*dIII- and *Sma*I-digested *swi6* fragment from the mutagenized *URA*+ pRS316 construct into the *LEU*+ pRS305 vector (*29*). The pRS305 vector was then linearized by digesting with *Hpa*I (or *Nar*I for BY2220, -2214, -2215, -2216, and -2217) and transplaced into the chromosomal *leu2* locus of the BY600 (*swi6*Δ) strain using targeted integration as described previously (*27*). Integrated mutants were placed under *LEU* selection, and transplacement was confirmed with both PCR and sequencing.

Immunoblotting. Yeast cell cultures were grown overnight at 30 °C in selective media to an OD_{660} of <0.5, then diluted to an OD_{660} of 0.2, and split and grown at either 25 or 37 °C for up to 10−12 h (OD_{660} of 0.4−0.5). Protein extracts were made by lysing the cells with glass beads under hypotonic conditions in extract buffer [100 mM Tris (pH 8.0), 20% glycerol, 0.1% Triton X-100, and 1 mM EDTA] in the presence of β-mercaptoethanol (10 mM) and protease inhibitors [PMSF (1 mM), leupeptin (1 μg/mL), and pepstatin A (1 μg/mL)]. The protein concentration of each extract was measured using the Bradford assay (*30*), and 100−200 μg of protein from each sample was boiled in SDS buffer [62 mM Tris-HCl (pH 6.8), 10% glycerol, 5 mM β-mercaptoethanol, and 3% SDS] and then run on a 10% polyacrylamide gel for 2.5−3 h. After semidry transfer of the protein to a nitrocellulose filter (MSI), the filter was blocked with TBST buffer [50 mM Tris-HCl (pH 7.5), 200 mM NaCl, and 0.05% Tween 20] containing 5% nonfat dry milk for 2 h. The filter was then probed with a rabbit polyclonal Swi6 antibody (1:700) and a goat anti-rabbit IgG secondary antibody conjugated with horseradish peroxidase (1:4000). The protein bands were detected using the ECL Western blotting detection system from Amersham.

Band Shifts. The plasmid pBD972 was used for in vitro translation of Swi4. It contains a 700 bp CITE (*31, 32*) and myc tag sequence insertion 5′ of the *SWI4* ATG codon and was constructed by inserting the *SWI4* gene into pBD939, which is a pBSKS+ vector with the CITE and myc tag sequence insertions between the *Apa*I and *Eco*RI restriction sites. To generate the wild-type Swi6 in vitro translation construct, pBD972 was used as a template for primers BL139 (5′CTCGAGTTCCATGGTTGTGGCC3′) and the M13 reverse primer to generate a 700 bp fragment containing the CITE sequence. After the PCR product was cloned into the pCRII vector (Invitrogen) (pBD2158), the CITE fragment was released by *Xho*I digestion and substituted for the 300 bp *Xho*I fragment of pBD1378, generating the wild-type *SWI6* CITE construct, pBD2090. Mutant allele *swi6*−*405* (pBD2091) and *swi6*−*406* (pBD2094) CITE constructs were

also generated through substitution of the 300 bp *Xho*I wild-type fragment with the 700 bp *Xho*I CITE fragment of pBD2158. The *Sac*I-digested wild-type *SWI6* vector (pBD2090) was ligated to the *Sac*I fragments containing the 3′ portions of the open reading frames of the PCR-generated and site-directed *swi6* mutant alleles to generate the mutant *swi6* CITE constructs. In vitro translation of both proteins was carried out as described in the general protocol for the Promega TNT Lysate Coupled Transcription/Translation Reactions. The lysate reaction was performed according to the manufacturer's recommendations. One-half of the reaction mixture was incubated with nonlabeled amino acids for 2.5 h at 30 °C. The other half of the reaction mixture was labeled with [^{35}S]methionine at 30 °C for 2.5 h, then run on a 10% polyacrylamide gel, and exposed overnight to determine the yield of both Swi4 and Swi6. Band-shift experiments were carried out as described previously (*3*) using 20−30 μg of whole cell extract with a $^{32}PO_4$-labeled 130 bp fragment of the *HO* promoter containing four SCB elements (−503 to −374 from the ATG). Band-shift reactions were performed at both 25 and 37 °C for 25 min. The reaction products were run on a 4% polyacrylamide nondenaturing gel for 3.5 h at 160 V, dried, and exposed overnight.

β-Galactosidase Activity. The X-gal filter and ONPG assays of β-galactosidase have been described previously (*21*). β-Galactosidase activity was normalized to protein levels using the following equation: 1000 × OD_{420} (per milliliter of supernatant)/protein concentration (milligrams per milliliter of supernatant) × reaction time (minutes). To compare SCB transcriptional activity levels to those of MCB-driven transcription, we generated *LEU+* constructs containing three tandem repeats of either SCB (pBD2128) or MCB (pBD2129) elements driving *CYC1:lacZ.* These constructs were generated from *URA+* plasmids pBD1390 (*21*) and pBD1166 (*33*), respectively, through conversion to *LEU+* using the "marker swap" plasmid pUL9 [procedure and construct described elsewhere (*34*)]. To analyze the PCR-generated mutants, we cotransformed pBD2128 or pBD2129 into the BY660 strain (*MATa, swi6::TRP1−197, ho, his3, ura3, leu2, trp1, can1−100, ade2, met*) with the *swi6* mutant allele on CEN *URA+* plasmids, described above. For the site-directed mutants, the *URA+* tandem repeat constructs pBD1390 and pBD1166 were transformed into the mutant yeast strains. After overnight growth on selective media, the cultures were diluted to an OD of 0.1, grown for 4−7 h to an OD of 0.5, and then handled as referenced above. Measurements were made from at least four cultures, and the data reported are average values. The variations between assays were less than 20%.

Generation of Single Mutant Subclones. The two mutations in plasmids *swi6−405* and *swi6−416* were separately subcloned as follows. Each plasmid was first linearized by digestion with either *Hin*dIII or *Sma*I. The *Hin*dIII linear fragment from each mutant was then digested with *Alw*NI to generate a 2330 bp fragment containing the isolated N500Y (*swi6−418*) mutation in the case of *swi6−405* and the A477T (*swi6−417*) mutation in the case of *swi6−416*. To generate the N330T (*swi6−425*) mutation from *swi6−405* or the N330K (*swi6−426*) mutation from *swi6−416*, both mutant plasmids were digested with *Sma*I first and then with *Alw*NI, yielding the 2270 bp fragment that contained either the N330T (from *swi6−405*) or the N330K (from *swi6−416*) mutation. Gel-purified mutant fragments were then ligated to the gel-purified complementary wild-type fragments of the *Sma*I−*Alw*NI-digested plasmid pRS316 (BD1378). *swi6−419* was created exactly as described above for mutants *swi6−417* and *−418*, using the *Hin*dIII-digested fragment of the parent plasmid *swi6−414*.

Table 1: Summary of Screen Results[a]

	PCR-generated mutants of Swi6		
	0.5 mM $MnCl_2$	0.25 mM $MnCl_2$	0.1 mM $MnCl_2$
complexity	300	1000	1000
total mutants isolated	82	7	18
temperature-sensitive mutants	18	5	12
nonconditional mutants	64	2	6
express SWI6	13	0	2
do not express SWI6	51	2	4

[a] Three separately generated ankyrin repeat mutant libraries, using different concentrations of $MnCl_2$, were screened for temperature sensitivity of Swi6 transcriptional activity using an SCB-carrying *ho:lacZ* reporter. Nonconditional, or null, mutants are defined as those that are not able to express *ho:lacZ* at either the permissive (25 °C) or the nonpermissive (37 °C) temperature. Expression of Swi6 by the nonconditional mutants was determined by immunoblotting cell extracts grown at 37 °C. Complexity represents the number of independent transformants obtained for each library.

RESULTS

Identification of Mutants in the Swi6 Ankyrin Domain Which Inactivate Swi6. To assess the importance of the *SWI6* ankyrin repeat domain for transcriptional activity, we used mutagenic PCR to specifically target mutations to this region. Using primers flanking the first and part of the fifth repeat, we generated three libraries that were independently mutagenized in the presence of 0.5, 0.25, and 0.1 mM $MnCl_2$ (*22*). In all screens, the libraries were transformed into a *swi6* deletion strain (BY600) carrying the *ho:lacZ-46* fusion at the chromosomal *HO* locus (*7*). Transformants were screened for β-galactosidase activity after growth at 25 and 37 °C. From the first screen of the most heavily mutagenized library (0.5 mM $MnCl_2$), we isolated 18 different temperature-sensitive alleles and 64 nonconditional, or null, alleles (Table 1). Of the nonconditional mutants, 51 did not express any Swi6 protein and had therefore acquired mutations that affected Swi6 stability or truncated the protein. We sequenced two of the 13 null alleles that expressed Swi6 and found that each contained at least four substitutions in the ankyrin repeat region. In contrast to the null alleles, all but one of the 18 temperature-sensitive mutants expressed *SWI6* at the nonpermissive temperature, although in most cells the level of Swi6 is slightly lower than that in cells bearing wild-type *SWI6* plasmids (data not shown). We know that, in contrast to Swi4, which is undetectable by immunoblotting and rate-limiting for G1 progression in heterozygotes (*3*, *35*), Swi6 is easily detected and its overproduction has no phenotypic effect. It is therefore unlikely that the Swi6 protein is limiting for cell cycle progression or that modest fluctuations in Swi6 levels would contribute significantly to the phenotype of these mutants. Four of the temperature-sensitive mutant plasmids, H323R, G347D, L474S, and N500T, have single base pair substitutions that map to

residues within the first, second, fourth, and fifth repeats, respectively. The other 11 mutant plasmids from screen 1 all contain two to four substitutions across the ankyrin repeat region (Figure 2).

In attempts to identify more single mutants, we sequenced temperature-sensitive mutants out of the less mutagenized (0.25 and 0.1 mM $MnCl_2$) libraries (screen 2). The total number of mutants found in these libraries was significantly less than the number identified in the 0.5 mM $MnCl_2$ library, despite the fact that these libraries had a higher complexity (Table 1). This suggests that the degree of mutagenesis was indeed decreased compared to that of the library generated in 0.5 mM $MnCl_2$. Several mutations were isolated multiple times within and across the three libraries, indicating that the libraries were screened to completion and that hot spots for mutation exist within this region. In particular, G347 was mutated at least 10 times, and both N330 and K441 were mutated at least four times. As observed in the first library (0.5 mM $MnCl_2$), the majority (six of eight) of the null alleles isolated from the other libraries (0.1 and 0.25 mM $MnCl_2$) did not express the Swi6 protein. In addition, we again observed that the majority of the temperature-sensitive *swi6* alleles contained two or more mutations within the ankyrin repeat domain.

We also screened the 0.5 mM library for partially active *SWI6* mutants (screen 3), characterized as blue at 25 °C and pale blue at the nonpermissive temperature of 37 °C, to determine whether additional single mutants might confer this less severe temperature-sensitive phenotype. With this less stringent criterion, we isolated the previously identified *swi6−405* allele, one single mutant (R344G), one double mutant (*swi6−423*), and three triple mutants (*swi6−420*, *−421*, and *−422*). Therefore, even a search for weakly defective ankyrin repeat mutants yielded a preponderance of plasmids with multiple mutations. The only single mutation that was obtained from this screen, R344G, has a substitution within the same region of the ankyrin domain as that of the G347D mutation, which was previously identified in the screen for temperature-sensitive alleles of this library.

The preponderance of double and triple mutations among plasmids screened for defects in transcription suggested that multiple mutations in the ankyrin domain might be required to alter the structure and/or function of Swi6. Alternatively, the multiple mutations might be an artifact of the PCR method of mutagenesis, in which case only one of the mutations would be responsible for the temperature-sensitive transcription defect. To distinguish between these two possibilities, and to analyze the potential for an additive phenotype between two mutations in different regions of the domain, we subcloned two single mutations into an otherwise wild-type Swi6 from each of two double mutants: *swi6−405* and *swi6−416*. The double mutants had mutations in the first and fourth (*swi6−416*) or the first and fifth (*swi6−405*) repeats. The two single mutants generated from the temperature-sensitive mutant *swi6−405*, *swi6−425* (N330T) and *swi6−418* (N500Y), had β-galactosidase levels (using a tandem triple SCB reporter construct) of 86 and 50%, respectively, and the original double mutant (*swi6−405*) had 38% activity. This indicates that the combination of both mutations results in a more defective Swi6 than either mutation alone and that, in the native structure, N330T has near wild-type activity. *swi6−426* (N330K) and *swi6−417* (A477T) were derived from *swi6−416*, which originally showed a moderately low level of activity (26%). In this case, the *swi6−426* single mutant appears to have a gain of function effect on transcriptional activity, showing 165% of wild-type activity with the triple SCB reporter construct, and *swi6−417* is moderately defective, allowing 30% of the transcriptional activity of Swi6. In contrast to the previous example, the combination of the two mutations gives an activity level approximating that of the *swi6−417* mutant in isolation, suggesting that the *swi6−426* gain of function mutation is far less efficient in the mutant background. These results show that substitution of N330 with T has little impact on the function of Swi6 in *HO* transcription whereas the substitution of K in that same position has a significant gain of function phenotype.

Including A477T, which we obtained by separating the two mutations found in *swi6−416*, we have identified six residues (marked with arrows in Figure 2) within the *SWI6* ankyrin domain that, when substituted, inactivate the SCB transcriptional function of *SWI6*. Interestingly, all six of these mutations cluster in the N- or C-terminal quarter of the ankyrin domain. Mutations were obtained within the central portion of the domain, but these mutants included additional mutations at either end or both ends of the domain. The only exception to this is *swi6−415*, which has two mutations six residues apart at the junction between the second and third repeats. This could indicate that the middle two repeats are less important and therefore mutationally silent. However, an equally plausible alternative is that the middle repeats are so crucial to Swi6 function and stability that these mutants were among the null mutants that produced no Swi6 protein and were not further characterized.

To test whether the inability of the Swi6 ankyrin mutant proteins to activate SCB transcription is due to a defect in the ability of the Swi4−Swi6 complex to bind DNA, we compared the DNA binding activities of these mutant proteins to that of wild-type Swi6 by band-shift analysis. Using whole cell extracts derived from the wild-type, *swi6−405*, and *swi6−406* strains and a fragment of the *HO* promoter as the SCB DNA probe, we find that the wild-type complex migrates predominantly as a single lower complex (Figure 3A). Extracts from the *swi6−406* strain contain a complex that binds DNA about as efficiently as wild type, but the complex formed migrates more slowly (referred to as the upper complex). The *swi6−405* extract produces both upper and lower complexes in approximately equal amounts. These differences in mobility could be due to differences in the protein composition of the complexes or to modification or conformational changes within the Swi4−Swi6 mutant complexes. The variations in steady state levels of Swi6 in the temperature-sensitive mutants compared with that in the wild type could also influence the amount and type of complexes that form.

To eliminate some of these complications, we have used in vitro translated Swi4 and Swi6 in the DNA binding reactions. All of the ankyrin repeat mutant plasmids, as well as the wild-type *SWI6* plasmid, were transcribed and translated and found to yield comparable levels of Swi4 and Swi6 protein products (Figure 3B and data not shown). DNA binding reactions using the in vitro translation products from *swi6−406* and wild-type *SWI6* plasmids were analyzed in

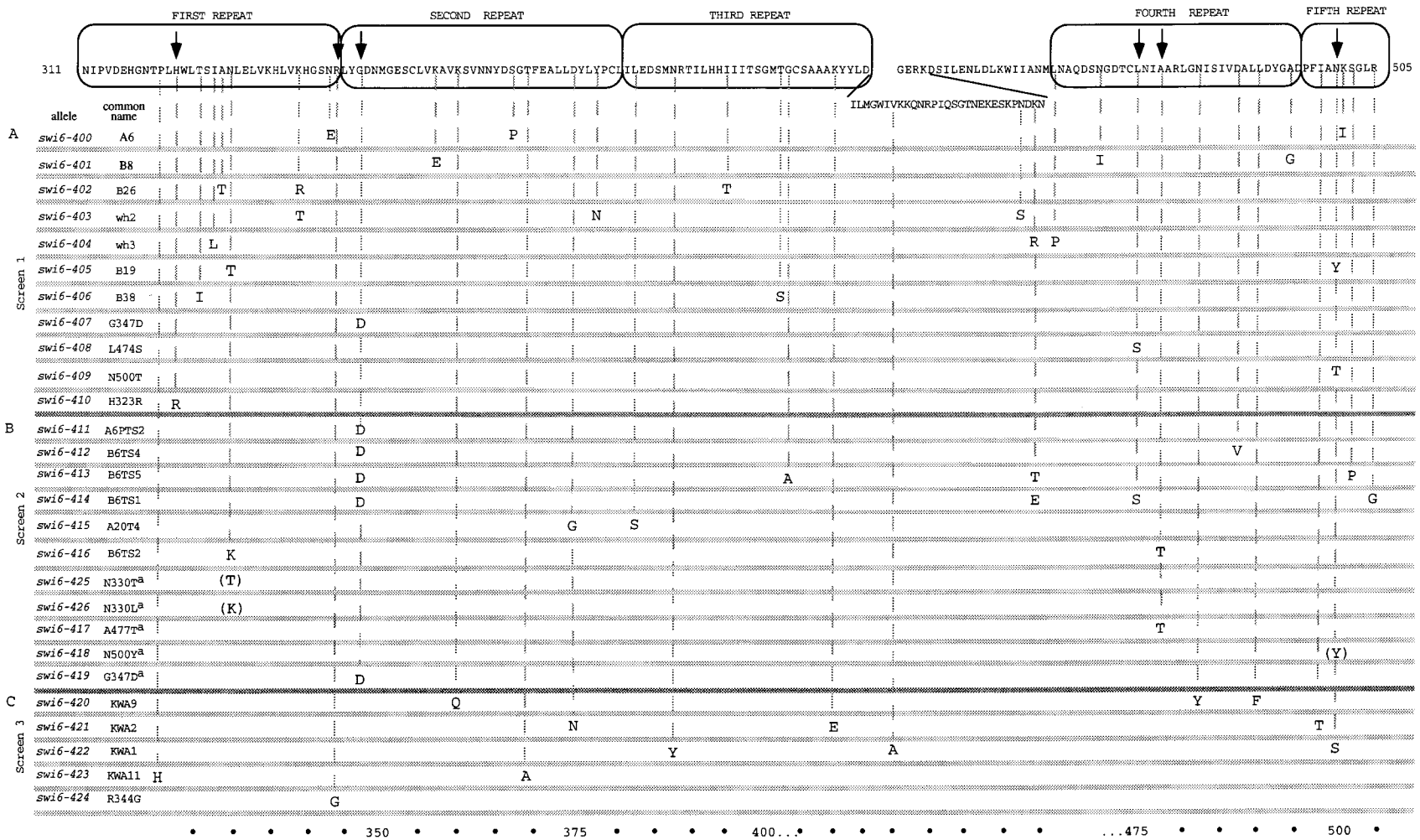

FIGURE 2: Ankyrin repeat region of Swi6 showing positions of residue substitutions. (A) Eleven PCR-generated temperature-sensitive mutants were isolated from the 0.5 mM $MnCl_2$ library after screening for *ho:lacZ* expression (screen 1). (B) The second group of mutants (screen 2) was isolated from both the 0.25 and the 0.1 mM $MnCl_2$ libraries. Only one mutant containing a single base pair substitution, G347D (*swi6−407*), was isolated from this screen. It was isolated four times as a single mutation and had been previously identified as a temperature-sensitive mutation in screen 1. [a]These mutations were derived from a parent plasmid that had been previously identified in either screen 1 or 2. The residues in parentheses indicate isolated substitutions that did not reduce Swi6 function when subcloned from the additional mutations originally identified in the parent plasmid (described in the text). (C) Mutants *swi6−420*, *−421*, *−422*, and *−423* and R344G (*swi6−424*) were isolated by screening the 0.5 mM $MnCl_2$ library for less severe temperature-sensitive mutants with the expectation that these would contain fewer mutations (screen 3). One additional mutant allele carrying a single R344G substitution was isolated from this screen. The arrows at the top of the figure indicate single-residue substitutions that confer a temperature-sensitive phenotype to Swi6, and the numbers at the bottom indicate the position of these mutations within the Swi6 protein sequence.

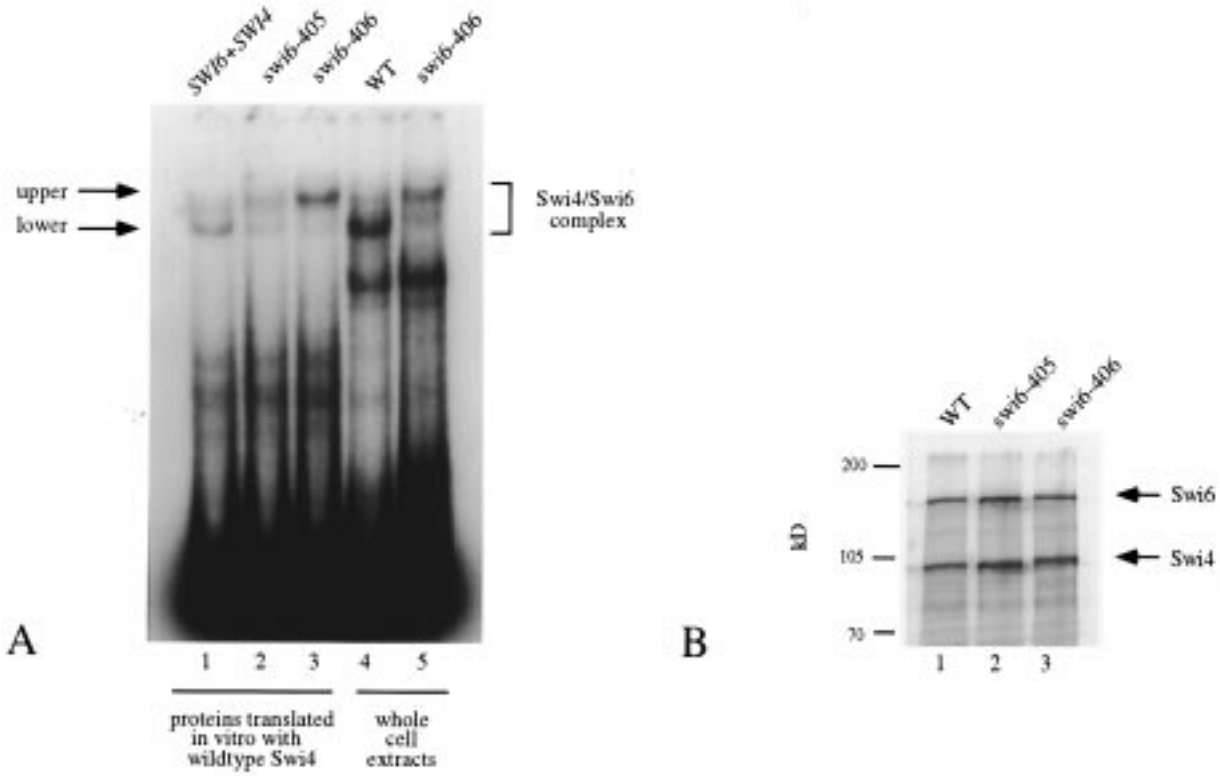

FIGURE 3: Band-shift comparison of *SWI6+* and mutant alleles using both in vitro translated proteins and whole cell extracts. (A) This band-shift gel shows comparable band-shift patterns with regard to upper and lower complex formation between a whole cell extract derived from a wild-type strain (lane 4) and in vitro translated Swi4 and Swi6 protein products (lane 1). A 130 bp fragment of the *HO* promoter, −503 to −374, was used as the DNA probe for the band-shift experiment which was performed at 25 °C. Lanes 1−3 contain proteins that were translated in vitro. Lanes 4 and 5 contain proteins expressed in whole cell extracts. Lane 1: Swi4 (pBD972) and Swi6 (pBD2090). Lane 2: Swi4 and *swi6−405* (pBD2091) (mutant protein showing both the upper and lower complex at 25 °C). Lane 3: Swi4 and *swi6−406* (pBD2094) (mutant protein showing a predominantly upper complex). Lane 4: wild type [BY600 transformed with *SWI6+* (pBD1378)]. Lane 5: *swi6−406* (pBD2046) expressed on a low-copy plasmid in the *swi6*Δ strain, BY600. (B) Both Swi4 and Swi6 are produced at comparable levels after in vitro translation (described in Experimental Procedures) at 30 °C. Lane 1: *SWI6+* (pBD2090). Lane 2: *swi6−405* (pBD2091). Lane 3: *swi6−406* (pBD2094). All other Swi6 mutants show similar expression levels in this reaction.

parallel with those produced from whole cell extracts. The resulting band-shift patterns are qualitatively similar [compare lanes 1 and 3 of Figure 3A (in vitro translation products) to lanes 4 and 5 (whole cell extracts)]. Since the in vitro translated Swi4 and Swi6 were the only yeast proteins added to the reaction mixtures in lanes 1−3, it is unlikely that the tendency of the *swi6−406* ankyrin repeat mutant to form upper complexes is due to binding of additional proteins to the DNA−protein complex. It is also unlikely that differences in protein modification are responsible, since the proteins are translated in a rabbit reticulocyte lysate system. The possibility that proteins in this lysate could bind or modify the yeast protein−DNA complex cannot be excluded, but to produce these results, the protein has to be specific for the swi6 mutant complexes. The protein would also need to be present in both rabbit and yeast cells, because the band shift is identical whether the mutant protein is translated in vitro or harvested from yeast.

To observe the extent of variation in DNA binding activity, the collection of temperature-sensitive ankyrin repeat mutants of Swi6 were translated in vitro and surveyed for DNA binding activity at two temperatures. Most of the Swi6 mutants retained the ability to complex with Swi4 and bind SCB elements at the nonpermissive temperature. Frequently, however, the mobility of the ankyrin mutant complex was noticeably altered (Figure 4) and migrated as an upper complex that could not be distinguished from that of *swi6−406*. The wild-type (*SWI6+)* band-shift pattern shows the predominant lower band at 25 °C and a more dispersed pattern, including both upper and lower complexes, at 37 °C. From the band-shift assay, the *swi6* mutants can be grouped into four categories. The first group of mutants [*swi6−406*, *−407* (G347D), and *−401*] all form the upper complex predominantly at both the permissive (25 °C) and nonpermissive (37 °C) temperatures. The second group of mutants [*swi6−405* and *swi6−410* (H323R), *−422*, *−421*, *−424* (R344G), *−402*, and *−417* (A477T)] form the upper complex at the nonpermissive temperature and both the upper and lower complex at the permissive temperature. The third phenotype is overall reduced binding, even at the permissive temperature, seen with mutants *swi6−401*, *−417*, and *−422*. The fourth group of mutants [*swi6−409* (N500T), *−415*, *−420*, *−423*, and *−418* (N500Y)] show no binding defect at either temperature. Most of the mutants show altered binding characteristics with a propensity to form the upper complex, which is exacerbated by elevated temperatures. A minority have reduced overall DNA binding. Formation of the upper complex therefore correlates with the loss of transcriptional activation, which is also enhanced at high temperatures. Despite the considerable variability in the DNA binding complexes formed, the upper complex that most of the mutants display migrates at a very similar position in the band-shift gel. Since this is not likely to be due to changes in protein composition or modification states,

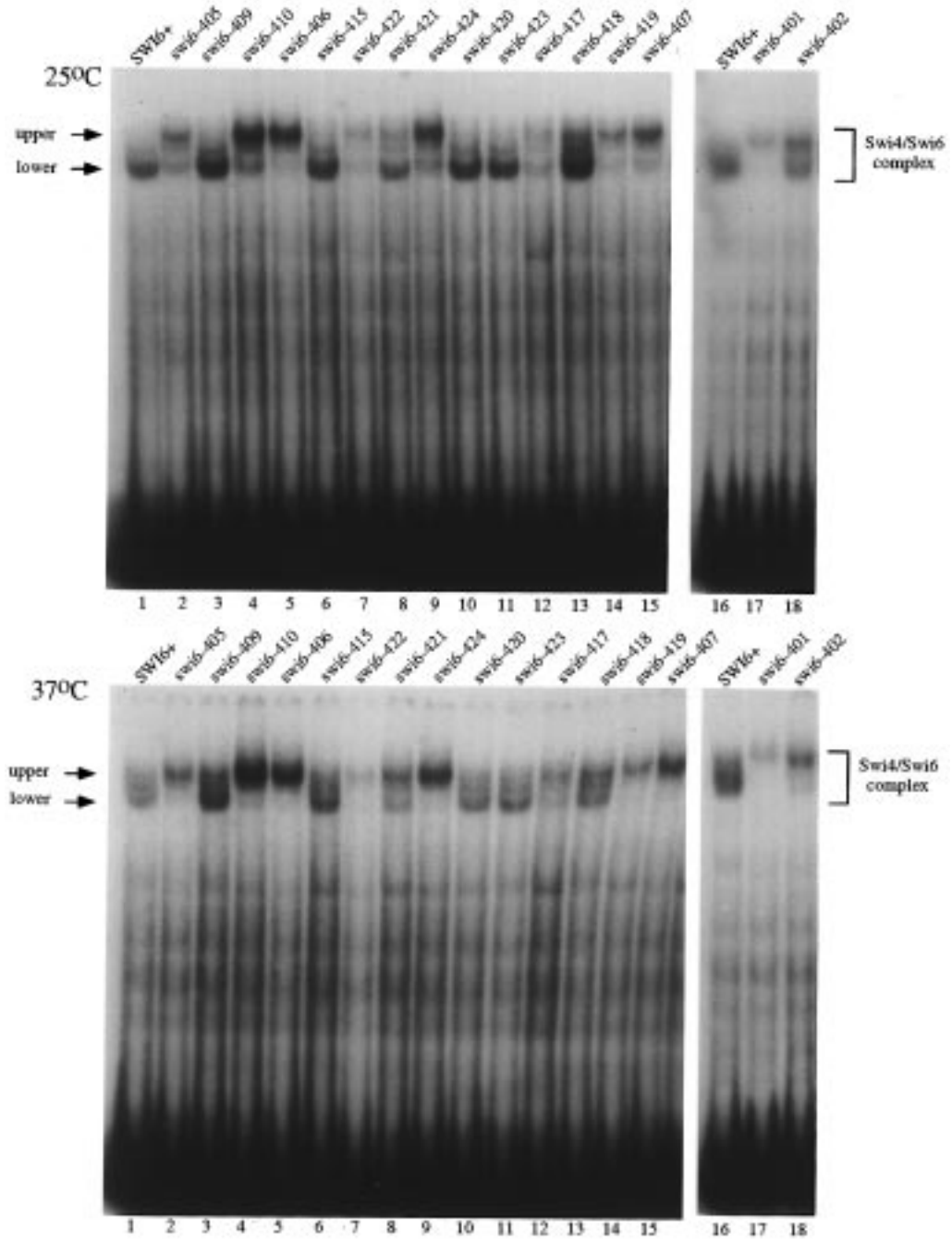

FIGURE 4: Band-shift patterns of in vitro translated wild-type and temperature-sensitive mutant *swi6* alleles. *SWI4* (pBD972) and the Swi6 plasmid indicated were translated in vitro and then used in band-shift reactions that were performed at either 25 °C (upper panel) or 37 °C (lower panel). The DNA target was a 130-base pair fragment of ^{32}P-labeled *HO* promoter containing three SCB elements. Five microliters of in vitro translation reaction product was included in each binding reaction mixture. Lanes 1 and 16: *SWI6+* (pBD2090). Lane 2: *swi6−405* (pBD2091). Lane 3: *swi6−409* (pBD2092). Lane 4: *swi6−410* (pBD2093). Lane 5: *swi6−406* (pBD2094). Lane 6: *swi6−415* (pBD2095). Lane 7: *swi6−422* (pBD2096). Lane 8: *swi6−421* (pBD2097). Lane 9: *swi6−424* (pBD2098). Lane 10: *swi6−420* (pBD2099). Lane 11: *swi6−423* (pBD2100). Lane 12: *swi6−417* (pBD2101). Lane 13: *swi6−418* (pBD2102). Lane 14: *swi6−419* (pBD2103). Lane 15: *swi6−407* (pBD2104). Lane 17: *swi6−401* (pBD2105). Lane 18: *swi6−402* (pBD2106).

we speculate that it may be the result of a global change in the conformational state of the Swi4−Swi6 complex which these mutations induce to varying degrees.

Effects of Alanine Substitutions in Core Residues of the Ankyrin Repeats of Swi6. To assess the importance and function of the individual ankyrin repeats, and because the significance of the middle repeats was still a question, we created mutations at equivalent sites in each of the four repeats. These mutations, substitution of alanines for each of the core residues (G-T-L in repeats 1 and 4, G-S-L in repeat 2, and N-T-L in repeat 3), eliminated the three most conserved residues in the repeats. In so doing, we hoped to completely disrupt the function of the conserved residues in each repeat in a similar manner. In addition, we created various combinations of the individual core region substitutions to determine whether any of these combinations would have additive effects. Immunoblots were performed on these strains as described earlier. Each of these site-directed mutants produces a detectable Swi6 protein product at 37 °C, although, like those of the PCR-generated mutants, the

Table 2: β-Galactosidase Activities for Swi6 Mutant Yeast Strains[a]

(strain) *SWI6* allele	repeats with core residues substituted	units of *ho:lacZ* activiity as a percentage of wild-type activity	
		25 °C	37 °C
(BY1379) *SWI6+*	−	34.0 (100)	23.0 (100)
(BY2220) *swi6−1000*	1	34.0 (100)	4.2 (18)
(BY2221) *swi6−200*	2	5.0 (15)	<0.15 (0)
(BY2222) *swi6−30*	3	1.5 (5)	<0.15 (0)
(BY2223) *swi6−4*	4	<0.15 (0)	<0.15 (0)
(BY2214) *swi6−1234*	1, 2, 3, 4	23.0 (70)	4.9 (21)
(BY2215) *swi6−123*	1, 2, 3	4.5 (14)	<0.15 (0)
(BY2216) *swi6−124*	1, 2, 4	4.6 (14)	<0.15 (0)
(BY2217) *swi6−134*	1, 3, 4	2.0 (6)	<0.15 (0)
(BY2218) *swi6−234*	2, 3, 4	4.2 (13)	<0.15 (0)
(BY2219) *swi6−23*	2, 3	5.8 (18)	1.6 (7)
(BY600) *swi6*Δ	−	<0.15 (0)	<0.15(0)

[a] β-Galactosidase levels for the site-directed mutants were determined using the *ho:lacZ* reporter construct. Each mutant was analyzed at least twice in duplicate, and results were calculated as a percentage of wild-type activity.

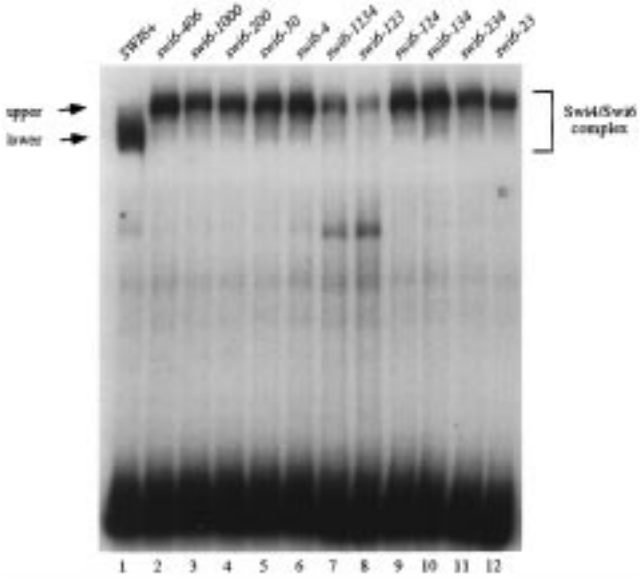

FIGURE 5: All Swi6 site-directed mutants bind SCB DNA elements in complex with Swi4 and form an exclusively upper band-shift complex. Band-shift experiments with in vitro translated Swi4 and Swi6 reveal the typical wild-type (WT) complex (lane 1), which shows the predominant lower complexes at 25 °C as indicated by the bracketed region. PCR-generated mutant *swi6−406* (lane 2) confers only the upper complex, as do all of the Swi6 site-directed mutants. The band-shift results shown are from a 25 °C binding experiment carried out as described in Figure 4. While the wild-type complex reveals a more distinct lower band at 25 °C, there was no difference in the Swi6 mutant band-shift results between the permissive and nonpermissive temperatures. Lane 1: *SWI6+* (pBD2090). Lane 2: *swi6−406* (pBD2094). Lane 3: *swi6−1000* (pBD2159). Lane 4: *swi6−200* (pBD2160). Lane 5: *swi6−30* (pBD2161). Lane 6: *swi6−4* (pBD2162). Lane 7: *swi6−1234* (pBD2163). Lane 8: *swi6−123* (pBD2164). Lane 9: *swi6−124* (pBD2165). Lane 10: *swi6−134* (pBD2166). Lane 11: *swi6−234* (pBD2167). Lane 12: *swi6−23* (pBD2168).

protein levels tend to be lower than that of the wild-type control. One surprising observation is that the mutants containing alanine substitutions within multiple cores attain a higher level of Swi6 protein than those mutants in which a single core region is alanine substituted (data not shown).

Using an integrated *ho:lacZ* reporter construct, we performed β-galactosidase assays to determine the transcriptional activity of these site-directed mutants. All of the core mutants displayed a temperature-sensitive phenotype in our most sensitive X-gal filter assay (*21*) of *ho:lacZ* expression (data not shown), and these results were confirmed by quantitative assays (Table 2). The four mutants that contain only one alanine-substituted core were all defective in *ho:lacZ* expression at the nonpermissive temperature. In the context of the native *HO* promoter, the fourth repeat appears to be the most critical for *HO*, or SCB-driven, transcription, showing severely defective transcriptional activity at both permissive and nonpermissive temperatures. There is no suggestion that any one of these repeats performs a function that is redundant. In addition, the fact that all of these mutants are temperature-sensitive suggests that the conserved residues within each repeat play critical roles in stabilizing the native structure of the Swi6 protein.

Another surprising property, revealed by combining these core substitution mutants, is that the *swi6−1234* allele, which contains mutations within the core residues of all four ankyrin repeats and was expected to be the most defective, has the highest level of β-galactosidase activity when compared with the other site-directed mutants (70% at 25 °C and 21% at 37 °C) using the *ho:lacZ* reporter construct. In contrast, substitutions within only the fourth core produce a highly defective protein, with no discernible β-galactosidase activity at the same temperatures. Apparently, substitutions within the three additional core regions produce a stabilizing or compensatory effect. The addition of substitutions within the first, second, and third core regions in varying combinations with the fourth also appears to increase activity compared to that seen with the single fourth core substitution at the permissive temperature, but not to the same extent as *swi6−1234*. One plausible explanation of this high level of activity could be that the ankyrin repeats are targets of negative regulation. In that case, loss of all four repeats would eliminate all targets of this repressive activity and would result in increased *ho:lacZ* expression. We cannot exclude this possibility, but we have monitored *ho:lacZ* transcription through the cell cycle in the *swi6−1234* strain and have found it to be cell cycle-regulated (data not shown). This indicates that negative regulation during the cell cycle still persists.

To measure the DNA binding defect associated with the core substitution mutants, we employed in vitro translation and band-shift assays as before, incubating the reaction mixtures at both 25 and 37 °C. As stated above, the wild-type Swi4−Swi6 complex exists as a combination of upper and lower complexes on SCB DNA, with a predominant lower complex at 25 °C. The core mutants all form the upper complex exclusively at both temperatures (Figure 5, 25 °C experiment shown). The ability to form the upper band-shift complex did not localize to mutations within a particular core region. Thus, even more so than with the PCR-generated repeat mutants, we see a dramatic but uniform shift in mobility of the DNA binding complex in the core mutants of Swi6. This, and the temperature sensitivity of all these mutants, suggests that the conserved core residues of all four repeats are important for maintaining the native structure of Swi6 and/or the Swi4−Swi6 complex.

Differential Effects upon SCB- versus MCB-Directed Transcription. We originally isolated the PCR-generated mutants because they were defective in transcription from the predominantly SCB-driven *ho:lacZ* promoter, so it was

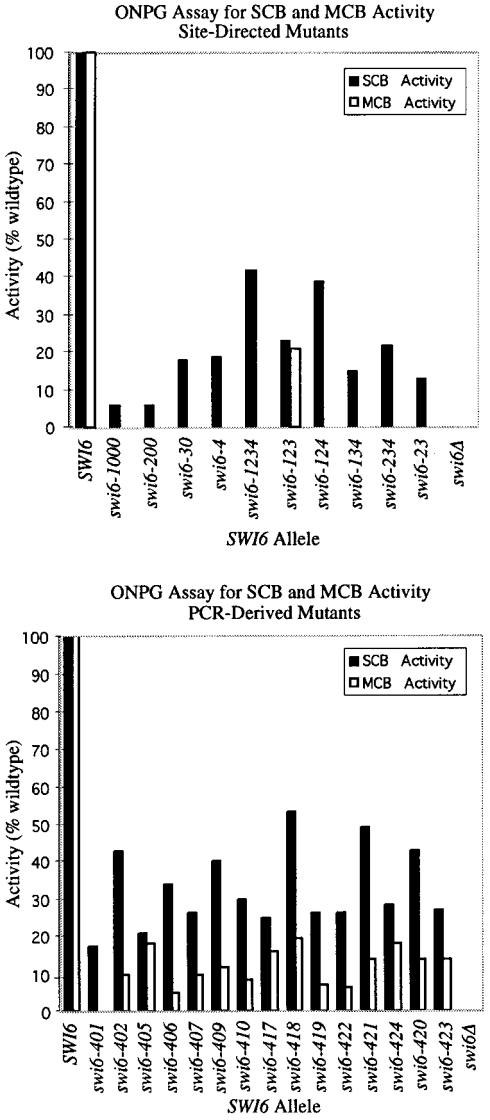

FIGURE 6: ONPG assay results for SCB and MCB reporter constructs. Using three tandem SCB (CACGAAAA) or MCB (ACGCGT) DNA binding elements driving the *LacZ* reporter, we measured the transcriptional activity (details in Experimental Procedures) of selected temperature-sensitive mutants. The activity is reported as a percent of the wild-type activity. The wild-type *SWI6* gene and each of the mutant alleles were on a low-copy plasmid in the presence of the reporter construct, which was expressed from a 2 μm plasmid.

of interest to measure the activities of these mutant proteins in MCB-driven transcription, which is activated by Swi6 bound to another partner, Mbp1 (*5*, *6*, *10*). To allow a direct comparison between SCB and MCB activation, we introduced a high-copy reporter construct carrying three tandem repeats of either MCB or SCB elements into the BY660 (*ho, swi6::TRP1−197*) strain carrying the mutant *swi6* allele on a low-copy plasmid (Figure 6). This enabled us to compare SCB and MCB activation within an equivalent context. Figure 6 shows that most of the PCR-derived and site-directed mutants cause a more severe MCB transcriptional defect when compared with SCB transcriptional activity. The most notable differences are seen with *swi6−1234*, which has 44% activity on SCBs and 0% on MCBs, *swi4−124*, which has 40% SCB activity and 0% MCB activity, and *swi6−421*, which has 48% of the wild-type SCB activity compared with 14% of the wild-type MCB activity. In addition, there are a number of mutants (*swi6−1000*, *−200*, *−123*, *−405*, *−417*, and *−424*) that show comparably decreased levels of both SCB and MCB activity when measured from these analogous promoter constructs. The fact that the vast majority of ankyrin repeat mutants are not equivalently defective with respect to MCB and SCB activation indicates there are differential effects upon the Swi4−Swi6 and Mbp1−Swi6 transcription complexes. This is somewhat surprising since the C termini, and not the ankyrin repeats of these proteins, are sufficient for the interaction between Swi6 and Swi4 (*3*, *4*) and between Swi6 and Mbp1 (*9*). Interestingly, all of the mutants are more defective in MCB activation than in SCB activation, despite the fact that they were selected for their inability to act at the *HO* promoter, which is activated by SCB elements. This suggests that the Swi6−Mbp1 interaction or activity has a stronger dependence either upon the ankyrin domain itself or upon other residues that are brought into proper position by the ankyrin domain structure.

Modeling Studies of the Ankyrin Repeat Mutations. The recent publication of the crystal structure of a p53 binding protein, 53BP2, which contains four ankyrin repeats (*17*), has enabled us to estimate the positions of the ankyrin repeat mutations of Swi6 that we have generated. First, the four ankyrin repeats of Swi6 and 53BP2 were aligned with 24 other ankyrin repeat domains using CLUSTAL-W (*36*). This multiple alignment provided a reliable means of aligning the two proteins' ankyrin repeats despite their low sequence identity (21%). Then, the coordinates for the 53BP2 structure, generously provided by N. P. Pavletich, were used in conjunction with the MODELLER program (*37*) to generate and refine a model of the Swi6 ankyrin domain. This model was strikingly similar to the 53BP2 structure. It was validated by three independent methods [PROCHECK, VERIFY-3D, and ERRAT (see the Figure 7 legend)], and all three indicated a high degree of reliability. The structure that 53BP2 adopts, and the one that the modeled Swi6 conforms to, resembles an "L" in profile, with continuous, tightly packed α-helices perpendicular to and connected by short β-hairpins. A ribbon diagram of the Swi6 ankyrin model structure is provided in Figure 7. The locations of the core residues and five single-point mutants are labeled. The regularity of this repeat structure is apparent in this view, as is the conserved positioning of the core residues in each repeat.

Alanine substitutions were made in the three most conserved core residues of the Swi6 ankyrin repeats in an effort to completely eliminate whatever function this repeating and conserved structure might have. These substitutions clearly disrupt Swi6 function, but because there are three changes in the structure in each repeat, it is not possible to be certain which of these substitutions is the most disruptive. However, sequence comparison with other ankyrin repeat-containing proteins, as well as inspection of the model of the Swi6 structure, suggests that the third substitution within the cores, which substitutes alanine for leucine at positions L322, L355, L392, and L474, is the most disruptive. First, while the glycine and threonine are conserved within the Swi6 family, these specific residues are not conserved in the ankyrin repeat family as a whole. In contrast, the leucine is highly conserved among the hundreds of ankyrin repeats that have been identified (*15*). In addition, inspection of the

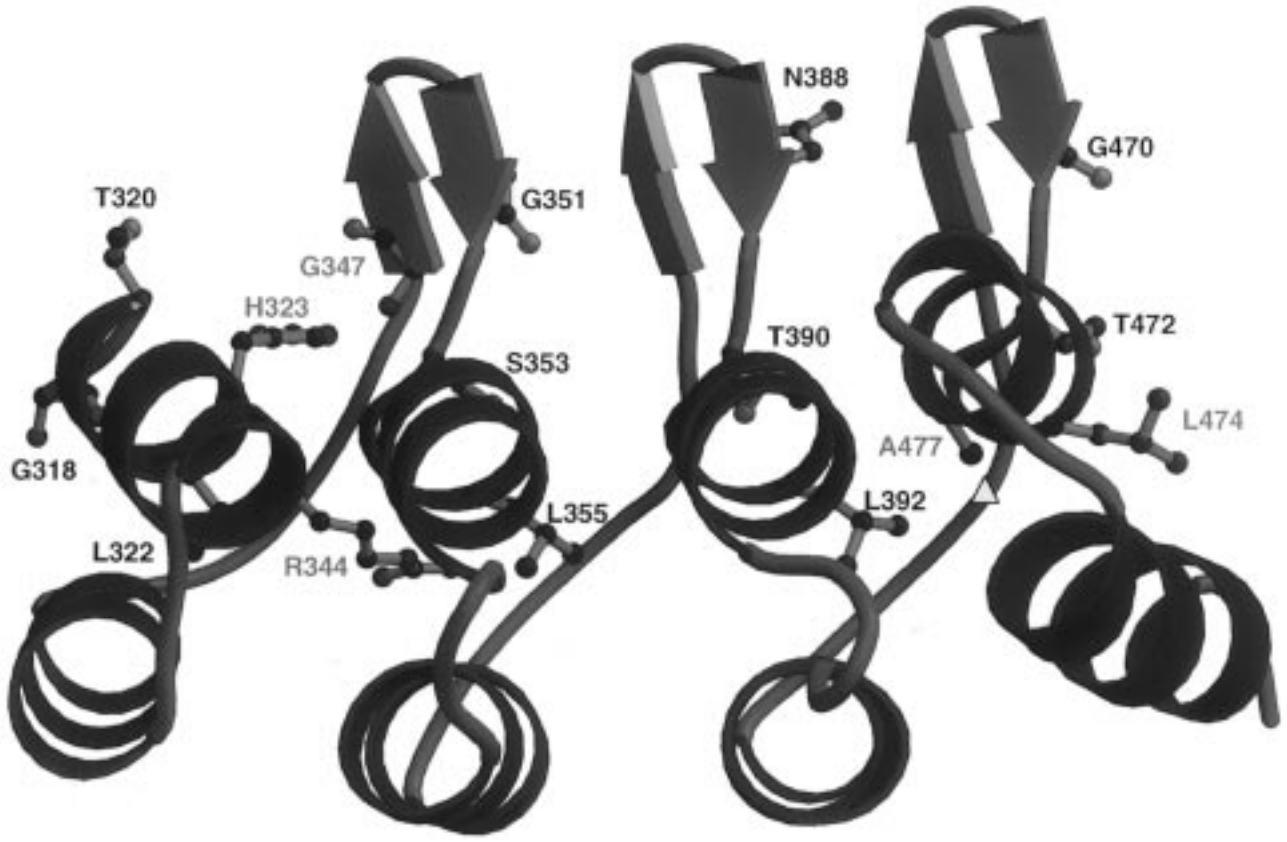

FIGURE 7: Ribbon diagram of the Swi6 ankyrin domain model. The model consists of three and one-half ankyrin repeats with the β-L-β-L-α-L-α motif. Here α-helix, β-strand, and loop (L) are color coded with blue, red, and green, respectively. The highly conserved core residues in the ankyrin repeats, G318, T320, L322, G351, S353, L355, N388, T390, L392, G470, and T472, and the single-site mutants generated in this study, H323, R344, G347, L474, and A477, are highlighted with ball-and-stick models. The single-site mutants are labeled in cyan, and the core residues are labeled in black, except for L474, which is a core residue that was also identified as a single mutant in our temperature-sensitivity screen. The color coding of the atoms is as follows: carbon, black; nitrogen, blue; and oxygen, red. Only the side chain atoms for each residue are shown in the ball-and-stick model except glycine where the main chain atoms are shown for easy identification. The model of the Swi6 ankyrin domain was derived from the crystal structure of a homologous ankyrin domain in the p53-binding protein (*17*) by the homology modeling method (*37*). Twenty-four sequences of ankyrin repeat domains were aligned by CLUSTAL-W (*36*) to achieve a reliable alignment of the Swi6 ankyrin domain with that of the p53-binding protein. The multiple alignment was required due to the low sequence homology between the ankyrin domains in Swi6 and the p53-binding protein. The initial model was generated and subsequently refined by MODELLER (*37*). The final model presented here was validated by PROCHECK (*45*), VERIFY_3D (*46*), and ERRAT (*47*). The result of PROCHECK showed that 99.1% of the main chain dihedral angles are within allowed regions. The rmsd bond length and angle are 0.02 Å and 2.47°, respectively. The average 3D_1D profile score for each residue is 0.34, with the lowest score of 0.24 for the N- and C-terminal residues as calculated from VERIFY_3D. ERRAT showed that 96.0% of the residues are within the 95% confidence limit. There are no residues above the 99% confidence limit level. These three independent validation methods suggest that the model is reliable. The long insertion between repeats 3 and 4 (residues 418−462) was excluded in the model, and a yellow triangle denotes the position of that undefined stretch in the structure.

Swi6 model shows that these leucines are part of a hydrophobic core which is likely to play a critical role in stabilizing the four α-helix bundles that are the predominant feature of the Swi6 ankyrin domain. The first of these three core leucines, L322, lies at the interface of four α-helices and is spaced appropriately to form tight hydrophobic interactions with three other hydrophobic residues in the adjacent helices (V334, V338, and L373). Leucine is often found to be a preferred residue in leucine zippers, coiled coils, and other structures in which α-helices are tightly packed (*38*), and in ankyrin repeats, they may also play a critical role in stabilizing the helix bundles.

Four ankyrin repeats occur in tandem within the yeast transcription factor family, and the four full repeats have been modeled on the basis of the structure of another protein which also contains four repeats. N500, one of the residues shown to be critical for Swi6 function in this analysis, is adjacent and C-terminal to the four-repeat structure. This asparagine, and the glycine that follows three residues downstream, are the residues that would be expected to begin a fifth repeat. However, the residues that follow do not conform to the consensus sequence. The significance of this partial fifth repeat is unclear, but the fact that it maintains appropriate spacing and sequence conservation within this family suggests that it may be important in the overall domain structure. This is corroborated by the fact that point mutations in N500 have been found which disrupt Swi6 function. In addition, there is another ankyrin repeat containing protein in yeast, Yar1, which also ends its ankyrin repeat sequence in the same manner (*39*).

Among the PCR-generated ankyrin repeat mutants, the most commonly identified mutation, isolated 10 times from three independent screens, was at the glycine G347 position and all were substitutions of glycine for aspartate (D). G347, as pictured in Figure 7, lies on the back surface of the modeled structure, in the β-hairpin connecting ankyrin

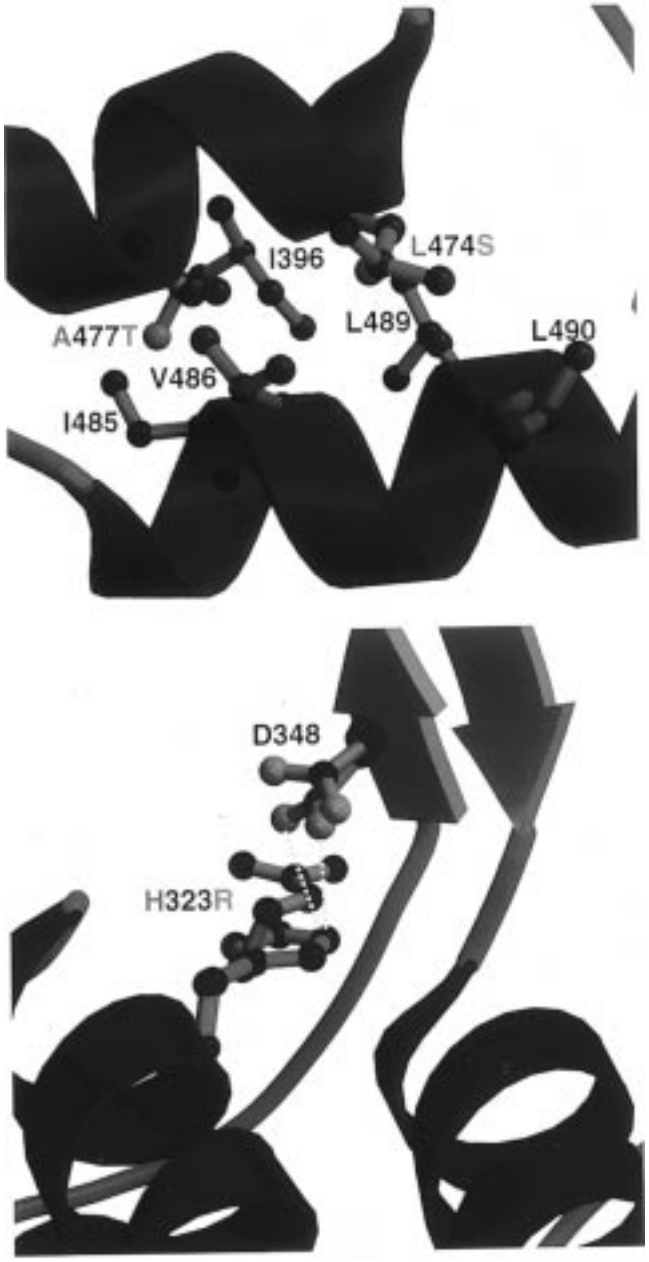

FIGURE 8: (A, top) Superposition of the two models of the L474S and A477T mutants where L474 and A477 in the wild type are substituted by Ser and Thr, respectively. The positions of mutant residues S474 and T477 were generated by MODELLER and subsequently refined. L474 and A477 and their neighboring residues, I396, I485, V486, L489, and L490 in the wild type as well as S474 and T477 in the mutant, are represented with ball-and-stick models. L474 and A477 in the wild type are indicated with a cyan bond color. Their neighboring residues in the wild type are indicated with a green bond color. L474 forms tight hydrophobic packing with the side chains of V486, L489, and L490, whereas A477 forms tight hydrophobic packing with I396, I485, and V486. In both mutants, the substitution of L474 by S474 and of A477 by T477 inserts a hydrophilic residue in the hydrophobic pocket, which will destabilize the four-α-helix bundle. (B, bottom) Model of the H323R mutant where H323 is substituted by Arg. The position of mutant residue R323 was generated by MODELLER and subsequently refined. Residue 323 and the neighboring D348 in the wild type and the mutant Swi6 are represented with ball-and-stick models and coded by their bond color of cyan and purple, respectively. The $N_{\epsilon 2}$ of H323 forms two hydrogen bonds indicated by yellow dashed lines with $O_{\delta 1}$ and $O_{\delta 2}$ of D348 in the wild type, whereas the guanidinium group of R323 in the mutant clashes with D348, although the side chain of D348 was pushed away from its wild-type position. This steric hindrance may lead to thermal instability of the mutant.

repeats 1 and 2. As such, changes at that position are unlikely to destabilize the structure itself. Rather, the loss of function that this mutation causes suggests that this residue may be part of a surface on which there is a critical interaction with another protein, or with another domain of the Swi6 protein. This is also likely to be the case for the gain of function mutation, N330K, which does not confer a conformational change to the modeled Swi6 ankyrin repeat.

The four other single mutations generated in this study that resulted in temperature-sensitive Swi6 proteins are all predicted to result in unfavorable interactions within the ankyrin repeat itself when modeled onto the structure. These findings help to validate the model and give us new insight into the key intramolecular interactions that occur in this structure. The core leucine (L) at position 474 changed to serine (S), and alanine (A) 477 changed to threonine (T) (Figure 8A); both disrupt the tight hydrophobic packing that is predicted to occur within neighboring residues. In the case of histidine (H) 323 (Figure 8B), which is replaced with arginine (R), the hydrogen bonds predicted to be formed by the histidine with aspartate (D) 348 are disrupted and the larger arginine side chain would be expected to perturb the local structure due to steric hindrance. Finally, the space filling models depicted in panels A and B of Figure 9 clearly show the effect predicted by substitution of R344 for glycine (G). In the model, the loss of the bulky side chain of the arginine creates a cavity on the surface of the structure which exposes the hydrophobic side chains of L322 and L373. This cavity is large enough to make this region accessible to water and would be expected to destabilize the structure.

DISCUSSION

Within the four ankyrin repeats in this family of transcription factors, three levels of conservation are observed. There are "core" residues, which are identical, as well as residues with chemical similarities that are conserved throughout all four of the repeats. Second, there are specific residues which are shared by repeats 1 and 4, making them much more similar to each other than the other repeats in these or any other set of ankyrin repeat proteins. Third, there are residues which are conserved within the individual repeats of all of the family members, but which differ widely between repeats. This study provides evidence that the core residues of all four of the repeats are important, but whether this is due to a structural requirement for a four-repeat domain or whether these repeats actually have different roles is unclear. The fact that the mutations in the core residues all result in temperature sensitivity and all cause what appears to be a dramatic conformational change in the Swi4−Swi6 DNA binding complex is evidence that the role of these residues may be structural.

Modeling studies of our single-point mutants also show that all but one of these mutations are likely to disrupt the structure of the ankyrin repeat domain. The one exception is G347D, which may define a surface on which there is a critical interaction. This interaction is most likely to be between Swi6 and Swi4, or with another part of Swi6, as this mutant also causes a dramatic shift in the ternary complex between Swi4, Swi6, and DNA on band-shift gels. Our transcript measurements show that all of the ankyrin repeat mutants, which were initially selected for defects in

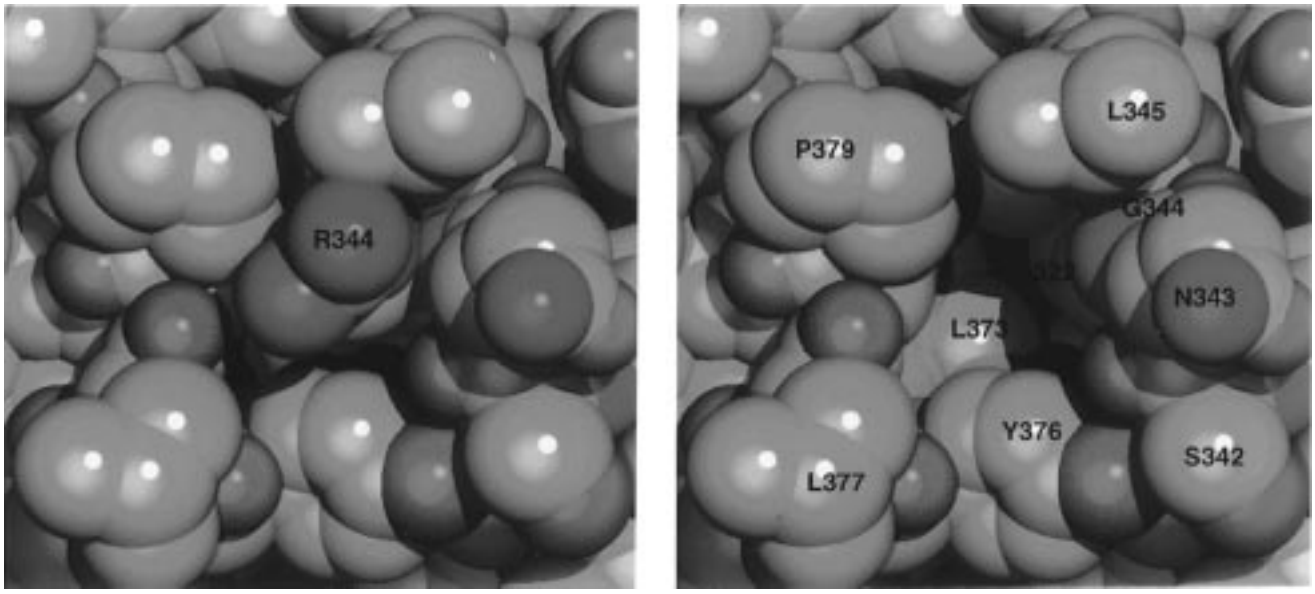

FIGURE 9: Space filling models of the wild-type Swi6 ankyrin domain in the region of R344 (A, left) and the mutant in the same region where R344 was replaced by G344 (B, right). The position of mutant residue G344 was generated by MODELLER and subsequently refined. The standard van der Waals radii were used to generate the spheres that represent all the atoms. The color coding is as follows: carbon, light green; nitrogen, blue; and oxygen, red. Panels A and B are viewed from the same orientation. Residue R344 in the wild-type Swi6 is labeled in panel A. Residue G344 in the Swi6 mutant and the neighboring residues are labeled in panel B. The substitution of R344 by G344 created a cavity in the mutant Swi6 and exposed the hydrophobic side chains L322 and L373. This R344G mutation will destabilize the Swi6 ankyrin domain due to the exposure of hydrophobic residues.

SCB-driven transcription in the context of the native *HO* promoter, have an even more severe defect in MCB-driven transcription. This greater dependence upon the ankyrin repeat domain for Mbp1−Swi6- than that for Swi4−Swi6-dependent transcription indicates differences in the contacts within the two complexes. These residues may be identifiable with more exhaustive genetic screens.

Ankyrin repeats were initially identified as statistically significant homologies between the repeats of Swi6 and its nearest *S. pombe* relative, Cdc10. Ankyrin repeats were also found in the Notch protein of *Drosophila* and the *Caenorhabditis elegans* lin-12 protein, both of which are also highly related (*1*). Since then, ankyrin repeats have been identified in more than 100 proteins with highly diverse functions (*15*). The sequence consensus has been relaxed considerably over that time, and the discovery of new members of the family is aided as much by the fact that they are nearly always present as tandem repeats as by their sequence similarities.

The function of the ankyrin repeat has been investigated in many different systems, and several key protein−protein interactions have been shown to depend on them (*40*−*44*). However, the repeats do not appear to interact with each other, nor has any other "signature" sequence been identified that is diagnostic of an ankyrin repeat-interacting protein. This, coupled with the fact that the proteins in which these ankyrin repeats are found have highly diverse functions and are located in a myriad of different cellular compartments (spider venoms, membrane transport proteins, and transcription factors), suggests that these repeats do not have a common function or binding partner. Rather, they should be viewed as structural units, which confer a particular type of protein fold. Gorina and Pavletich (*17*) have noted that ankyrin repeats form a novel L-shaped structure. Our study provides evidence that the conserved residues within each repeat are required to produce this structure, and as such, they provide a scaffold upon which different residues can be displayed. It is most likely that the nonconserved residues, which are unique to the different classes of ankyrin repeat-containing proteins, are responsible for specific interactions with other proteins and for providing the biological specificity and function to the ankyrin repeat proteins. The conserved residues, which are the defining feature of an ankyrin repeat, may play a strictly conformational function. Thus, the ankyrin repeat may be more appropriately viewed as a novel type of protein fold which provides a stable structure with surfaces that can be tailored for many different macromolecular interactions. Our data indicate that the ankyrin repeats of Swi6 are critical for the thermostability of Swi6 and for maintaining the proper conformation of the ternary complex between Swi4, Swi6, and DNA. It is still possible that the unique faces of the Swi6 ankyrin repeat domain form a binding site for another protein that has not yet been identified. However, it is more likely that these repeats provide a rigid structure that holds the Swi4−Swi6 complex in a precise and functional spatial arrangement with respect to the DNA.

ACKNOWLEDGMENT

We gratefully acknowledge N. Pavletich for providing the 53BP2 coordinates and M. Jurica, B. Stoddard, and members of the Breeden laboratory for helpful discussions and comments about the manuscript.

REFERENCES

1. Breeden, L., and Nasmyth, K. (1987) *Nature 329*, 651−654.
2. Lux, S. E., John, K. M., and Bennett, V. (1990) *Nature 344*, 36−42.
3. Sidorova, J., and Breeden, L. (1993) *Mol. Cell. Biol. 13*, 1069−1077.
4. Andrews, B. J., and Moore, L. A. (1992) *Proc. Natl. Acad. Sci. U.S.A. 89*, 11852−11856.

5. Koch, C., Moll, T., Neuberg, M., Ahorn, H., and Nasmyth, K. (1993) *Science 261*, 1551−1557.
6. Lowndes, N. F., Johnson, A. L., Breeden, L., and Johnston, L. H. (1992) *Nature 357*, 505−508.
7. Breeden, L., and Nasmyth, K. (1987) *Cell 48*, 389−397.
8. Ogas, J., Andrews, B. J., and Herskowitz, I. (1991) *Cell 66*, 1015−1026.
9. Dirick, L., Moll, T., Auer, H., and Nasmyth, K. (1992) *Nature 357*, 508−513.
10. McIntosh, E. M., Atkinson, T., Storms, R. K., and Smith, M. (1991) *Mol. Cell. Biol. 11*, 329−337.
11. Primig, M., Sockanathan, S., Auer, H., and Nasmyth, K. (1992) *Nature 358*, 593−597.
12. Andrews, B. J., and Herskowitz, I. (1989) *Nature 342*, 830−833.
13. Andrews, B. J., and Moore, L. (1992) *Biochem. Cell Biol. 70*, 1073−1080.
14. Partridge, J. F., Mikesell, G. E., and Breeden, L. L. (1997) *J. Biol. Chem. 272*, 9071−9077.
15. Bork, P. (1993) *Proteins: Struct., Funct., Genet. 17*, 363−374.
16. Tevelev, A., Byeon, I. L., Selby, T., Ericson, K., Kim, H., Kraynov, V., and Tsai, M. (1996) *Biochemistry 35*, 9475−9487.
17. Gorina, S., and Pavletich, N. P. (1996) *Science 274*, 1001−1005.
18. Reymond, A., Schmidt, S., and Simanis, V. (1992) *Mol. Gen. Genet. 234*, 449−456.
19. Siegmund, R. F., and Nasmyth, K. A. (1996) *Mol. Cell. Biol. 16*, 2647−2655.
20. Breeden, L. (1996) in *Start-specific transcription in yeast* (Farnham, P. J., Ed.) Vol. 28, pp 95−127, Springer-Verlag, Berlin.
21. Breeden, L., and Nasmyth, K. (1985) *Cold Spring Harbor Symp. Quant. Biol. 50*, 643−650.
22. Cadwell, R. C., and Joyce, G. F. (1992) *PCR Methods Appl. 2*, 28−33.
23. Sidorova, J., Mikesell, G., and Breeden, L. (1995) *Mol. Biol. Cell 6*, 1641−1658.
24. Kunkel, T. A. (1985) *Proc. Natl. Acad. Sci. U.S.A. 82*, 488−492.
25. Kraft, R., Tardiff, J., Krauter, K. S., and Leinwand, L. A. (1988) *BioTechniques 6*, 544−546.
26. Gietz, D., St. Jean, A., Woods, R. A., and Schiestl, R. H. (1992) *Nucleic Acids Res. 20*, 1425.
27. Orr-Weaver, T. L., Szostak, J. W., and Rothstein, R. J. (1981) *Proc. Natl. Acad. Sci. U.S.A. 78*, 6354−6358.
28. Breeden, L., and Mikesell, G. (1991) *Genes Dev. 5*, 1183−1190.
29. Sikorski, R. S., and Hieter, P. (1989) *Genetics 122*, 19−27.
30. Bradford, M. M. (1976) *Anal. Biochem. 72*, 248−254.
31. Elroy-Stein, O., Fuerst, T. R., and Moss, B. (1989) *Proc. Natl. Acad. Sci. U.S.A. 86*, 6126−6130.
32. Parks, G. D., Duke, G. M., and Palmenberg, A. C. (1986) *J. Virol. 60*, 376−384.
33. Lowndes, N. F., Johnson, A. L., and Johnston, L. H. (1991) *Nature 350*, 247−248.
34. Cross, F. R. (1997) *Yeast 13*, 647−653.
35. McInerny, C. J., Partridge, J. F., Mikesell, G. E., Creemer, D. P., and Breeden, L. L. (1997) *Genes Dev. 11*, 1277−1288.
36. Thompson, J. D., Higgins, D. G., and Gibson, T. J. (1994) *Nucleic Acids Res. 22*, 4673−4680.
37. Sali, A., and Blundell, T. L. (1993) *J. Mol. Biol. 234*, 779−815.
38. Alber, T. (1992) *Curr. Opin. Genet. Dev. 2*, 205−210.
39. Lycan, D. E., Stafford, K. A., Bollinger, W., and Breeden, L. L. (1996) *Gene 171*, 33−40.
40. Gu, Y., Turck, C. W., and Morgan, D. O. (1993) *Nature 366*, 707−710.
41. Kamb, A., Gruis, N. A., Weaver-Feldhaus, J., Liu, Q., Harshman, K., Tavitgian, S. V., Stockert, E., Day, R. S., Johnson, B. E., and Skolnick, M. H. (1994) *Science 264*, 436−440.
42. Bours, V., Franzoso, G., Azarenko, V., Park, S., Kanno, T., Brown, K., and Siebenlist, U. (1993) *Cell 72* (5), 729−739.
43. Nolan, G. P., and Baltimore, D. (1992) *Curr. Opin. Genet. Dev. 2*, 211−220.
44. Hatada, E. N., Nieters, A., Wulczyn, F. G., Naumann, M., Meyer, R., Nucifora, G., McKeithan, T. W., and Scheidereit, C. (1992) *Proc. Natl. Acad. Sci. U.S.A. 89*, 2489−2493.
45. Laskowski, R. A., MacArthur, M. W., Moss, D. S., and Thornton, J. M. (1993) *J. Appl. Crystallogr. 26*, 283−291.
46. Lüthy, R., Bowie, J. U., and Eisenberg, D. (1992) *Nature 356*, 83−85.
47. Colovos, C., and Yeates, T. O. (1993) *Protein Sci. 2*, 1511−1519.

BI972652E